Australian dust storms in 2002–2003 and their impact on Southern Ocean biogeochemistry

A. J. Gabric,[1] R. A. Cropp,[1] G. H. McTainsh,[1] B. M. Johnston,[1] H. Butler,[2] B. Tilbrook,[3] and M. Keywood[4]

Received 14 April 2009; revised 9 November 2009; accepted 14 December 2009; published 30 April 2010.

[1] During late 2002 and early 2003, southern Australia was in the grip of drought and experienced one of its most active dust storm seasons in the last 40 years with large dust plumes frequently advected over the adjacent Southern Ocean. We use meteorological records of dust activity, satellite ocean color, and aerosol optical depth data and dust transport modeling to investigate the transport and deposition of mineral dust from Australia over adjacent ocean regions and to correlate it with biological response in phytoplankton standing stock as measured by chlorophyll *a* concentration in 5 degree latitude bands from 40° to 60°S. Seasonal maxima in mean surface chlorophyll *a* of ~0.5 mg m^{-3} were not achieved until late January 2003 or during February in the more southerly bands, which when compared with a 9 year satellite mean climatology suggests the phenology of the bloom in 2002–2003 was atypical. Contemporaneous field data on CO_2 fugacity collected on transects between Tasmania and Antarctica show that significant atmospheric CO_2 drawdown occurred as far south as 60°S during February 2003. Our results provide strong evidence for a large-scale natural dust fertilization event in the Australian sector of the Southern Ocean and highlight the importance of dust-derived nutrients in the marine carbon cycle of the Southern Ocean.

Citation: Gabric, A. J., R. A. Cropp, G. H. McTainsh, B. M. Johnston, H. Butler, B. Tilbrook, and M. Keywood (2010), Australian dust storms in 2002–2003 and their impact on Southern Ocean biogeochemistry, *Global Biogeochem. Cycles*, *24*, GB2005, doi:10.1029/2009GB003541.

1. Introduction

[2] The Southern Ocean (SO) warrants investigation both as the prime global "High-Nutrient–Low-Chlorophyll" (HNLC) region and because of its pivotal role in global climate. The SO meridional overturning circulation contributes substantially to the global transport of climatically significant quantities such as heat, fresh water, nutrients, and anthropogenic CO_2 [*Marinov et al.*, 2006; *Sarmiento et al.*, 1998]. The aeolian supply of micronutrients to the global ocean is a key control on marine primary production, none more so than in southern hemisphere oceanic regions adjacent to arid continental regions, such as Patagonia and Australia [*Cropp et al.*, 2005; *Jickells et al.*, 2005]. Indeed, in HNLC regions such as the SO, dust-borne iron (Fe) is thought to limit primary production, control phytoplankton species composition, and potentially control the transfer of carbon to the deep ocean; thus affecting atmospheric CO_2 concentrations [*Ridgwell*, 2002]. Recent modeling analyses suggest that interannual variation in air-sea CO_2 fluxes in the past decade may be explained by variability in dust emissions that relaxes or increases Fe limitation in HNLC ocean regions [*Patra et al.*, 2007].

[3] Natural dust fertilization events have only rarely been documented [*Bishop et al.*, 2002], however, artificial Fe fertilization experiments in the SO (SOIREE at 61°S, EisenEx at 48°S and SOFex at 55°S and 66°S) demonstrated that raising the Fe level in the water by a few nanomoles per liter produced a significant increase in column-integrated phytoplankton biomass [*Bakker et al.*, 2005; *Boyd and Law*, 2001; *Coale et al.*, 2004; *Gervais et al.*, 2002]. Changes also occurred in the pelagic ecosystem structure, and in the cycling of carbon, silica and sulfur, such as a 10% drawdown of surface CO_2 [*Turner et al.*, 2004; *Watson et al.*, 2000]. During SOIREE, large diatoms accounted for up to 75% of primary production and were probably responsible for most of the observed 35–40 μatm decrease in pCO_2. Concurrent satellite data collected during SOIREE suggest the bloom was long-lived, persisting for over 40 days after the initial fertilization, however the final fate of the fixed algal carbon in both experiments could not be determined [*Bakker et al.*, 2001; *Boyd and Law*, 2001].

[1]School of Environment, Griffith University, Nathan, Queensland, Australia.
[2]Department of Mathematics and Computing, University of Southern Queensland, Toowoomba, Queensland, Australia.
[3]CSIRO Marine and Atmospheric Research, Hobart, Tasmania, Australia.
[4]CSIRO Marine and Atmospheric Research, Aspendale, Victoria, Australia.

0886-6236/10/2009GB003541

[4] These field experiments demonstrated iron's pivotal role in controlling carbon uptake and regulating atmospheric partial pressure of carbon dioxide, but were not able to determine the final fate of the algal carbon fixed during the bloom. Notwithstanding the results of these artificial fertilization experiments, the impact of natural dust deposition events on ocean biogeochemistry is still a topic of debate in the literature [e.g., *Boyd and Mackie*, 2008; *Cassar et al.*, 2007, 2008]. In a recent review, *Boyd et al.* [2010] suggest that there are only a few cases in which a causative link between dust supply and biological response can be found.

[5] The bioavailability of Fe in the ocean requires it to be in a soluble form, and Fe in mineral dust is typically insoluble [*Mackie et al.*, 2008]. Aerosol chemical composition is likely to be an important factor for the enhancement of iron fractional solubility through acid processing, but is difficult to substantiate from field data [*Baker and Croot*, 2010]. There is evidence for a complex biogeochemical link between Fe in aerosol and both anthropogenic SO_2 emissions [*Meskhidze et al.*, 2003] and biogenic sulfur (viz. dimethylsulfide, DMS) produced by marine phytoplankton [*Zhuang et al.*, 1992, 2003]. *Jickells and Spokes* [2001] report that overall solubility of aerosol Fe at seawater pH is 0.8%–2.1% of the total Fe deposited, however wet deposited mineral aerosols had a much higher soluble Fe than dry deposited (14%). When dust particles encounter more acidic cloud droplets and become incorporated in precipitation, Fe in dust may undergo dissolution as the soluble ferrous form, Fe II [*Behra and Sigg*, 1990; *Hsu et al.*, 2010], which would increase its bioavailability upon delivery to the ocean surface. Analysis of an 8 year time series of atmospheric measurements at Cape Grim, Tasmania (40°41′ S, 144°41′E) in the north of our study region, has confirmed the connection between atmospheric biogenic DMS and aerosol sulfur species, such as methanesulfonic acid (MSA), [*Ayers et al.*, 1991], so the potential for increasing Fe solubility certainly exists.

[6] The Australian continent has been recognized as a potentially important site for the study of terrestrial dust inputs to the SO and their impact on the marine food web [*Boyd et al.*, 2004; *Gabric et al.*, 2002; *Mahowald et al.*, 1999; *Rotstayn et al.*, 2009]. The Fe content of Australian dust is similar to Saharan dust [*Bonnet and Guieu*, 2004; *Mackie et al.*, 2008]. Model simulations suggest that aeolian dust from Australia dominates the Southern Hemisphere (SH) [*Tanaka and Chiba*, 2006], and there is evidence from other studies that episodic inputs of Australian dust exert an important influence on the continent's adjacent marine ecosystems [*Gabric et al.*, 2002; *Gingele and De Deckker*, 2005; *Shaw et al.*, 2008]. Although Patagonia is thought to be the main source of dust in Antarctic ice cores, recent isotopic analyses show that the dust from the Lake Eyre region of Australia could have been transported as far as the interior of the East Antarctic Plateau during present and past interglacial periods [*Revel-Rolland et al.*, 2006].

[7] The main pathway of dust leaving the Australian continent, is south over the Southern Ocean in association with the west-to-east passage of cold fronts and to the southeast, over the Tasman Sea. Dust is entrained by warm prefrontal northerly winds, frontal westerlies and postfrontal southerlies [*McGowan et al.*, 2000]. During spring and summer, the northerly migration of the band of cold fronts contributes to increased dust storm activity over southeastern Australia [*McTainsh et al.*, 1998]. Indeed, there is a strong seasonality in monthly average dust storm frequency related to wind conditions, rainfall, and vegetation patterns, with peak dust storm activity in southern Australia occurring during spring and summer [*McTainsh and Leys*, 1993]. The 2002–2003 spring-summer season in southern Australia was characterized by several high-intensity dust events, some of which were unprecedented in the dust storm record [*McTainsh et al.*, 2005]. There is as yet no detailed quantitative analysis of the impact of individual dust deposition events on the SO south of Australia, although the observed biogeochemical response during early 2003, was consistent with a hypothesis of dust deposition affecting ocean biogeochemistry [*Breviere et al.*, 2006].

[8] Global modeling analyses suggest that the SO dominates the present-day air-sea flux of anthropogenic CO_2, with one third to one half of the global uptake occurring south of 30°S [*Orr et al.*, 2001]. The subantarctic zone (SAZ, circa 40°–50°S) lies between the Subtropical Convergence (STC) and the subantarctic front (SAF), and is considered one of the strongest oceanic sinks for atmospheric CO_2 [*Takahashi et al.*, 2002]. Observations in our study region show that a strong CO_2 sink develops in the Austral summer (fugacity gradient, $\Delta fCO_2 < -50$ μatm) in the SAZ south of Australia (110°–150°E) [*Metzl et al.*, 1999]. The sink results from high winds and seasonally low sea surface fugacity of CO_2, relative to atmospheric fugacity (fCO_2). This sink is also associated with increased phytoplankton growth subsequent to the formation of a shallow summer mixed layer (about 100 m). The region of the SAZ, and immediately south, is also subject to mode and intermediate water formation, providing an important mechanism for transporting anthropogenic CO_2 into the ocean interior [*Metzl et al.*, 1999]. A strong CO_2 sink formed during February 2003, associated with an increase in phytoplankton biomass. *Breviere et al.* [2006] suggest this sink could not be explained by observed changes in mixed layer depth (MLD), wind speed, sea surface temperature (SST) or UV radiation, but might be explained by episodic atmospheric dust inputs.

[9] The paleoclimatic evidence is ambivalent in terms of the nexus between dust inputs, primary productivity and the carbon cycle [*Broecker and Henderson*, 1998; *Johnston and Alley*, 2006; *Ridgwell and Watson*, 2002]. Although it is well accepted that the ocean acts as a major sink for atmospheric CO_2 during glacial periods, and as a source of CO_2 to the atmosphere during glacial-interglacial transitions, the mechanisms responsible for determining the sign of the net exchange of CO_2 between the ocean and the atmosphere remain unresolved [*Michard*, 2008; *Raven and Falkowski*, 1999]. The interpretation of paleosedimentary records of marine productivity can be divergent, with some studies suggesting that neither changes in nutrient utilization in the Southern Ocean nor shifts in plankton dominance can explain the magnitude of CO_2 drawdown that occurred during the glacial/interglacial transition [*Kohfeld et al.*, 2005], while others point to massive increase in phyto-

plankton production during the last glacial, related to increased dust and Fe inputs [*Abelmann et al.*, 2006].

[10] Studies of Antarctic ice cores infer that during the last glacial maximum, dust-derived Fe depositional fluxes to the SO were an order of magnitude greater than the mean Holocene value [*Edwards et al.*, 2006, 1998; *Wolff et al.*, 2006], with high dust periods closely associated with abnormally low atmospheric CO_2 and temperature. Sedimentary core records of the last 50 kyr in the SO indicate that aeolian Fe inputs possibly switched diatom physiology toward higher carbon to silica and nitrogen to silica uptake and storage south of the SAF due to the dependency of photosynthesis on Fe levels [*Crosta et al.*, 2005]. The same ice core data point to large secular variations in atmospheric Fe supply during the 20thC that are likely to have had profound impacts on variability in primary production and ecosystem structure in Antarctic waters, and have been linked to the occurrence of periodic droughts (with increased dust storm activity) in Australia [*Edwards and Sedwick*, 2001].

[11] Here we present the first detailed analysis of what appears to be a natural ocean fertilization event in the SO south of Australia during the especially active dust storm season in the spring-summer of 2002–2003. We examine the impact of dust deposition to the ocean surface on phytoplankton biomass (indicated by surface chlorophyll) and the relation with measured atmospheric carbon drawdown. We have simulated atmospheric dust load and deposition over the ocean using a regional dust transport model that provides daily data from November 2002 to February 2003. The model results are supplemented with concurrent satellite data on aerosol optical depth (AOD), surface chlorophyll *a* (CHL), as well as field observations on dust storm activity and measurements of CHL and CO_2 partial pressures, collected on six cruises between Australia and Antarctica during the study period.

2. Methods

[12] For all analyses described here the study region is the SO south of Australia, between 40°–60°S and 135°–150°E for the time period November 2002 to February 2003.

2.1. Dust Storm Intensity Data

[13] The reduction in atmospheric visibility during a dust storm, or other dust entrainment event, is referred to as dust visibility reduction (DVR), and this can be used as a quantitative measure of the intensity of an event. This approach avoids the problems that can arise from incorrect dust event coding. DVR is calculated as follows:

$$DVR = V_{max} - V_{rec}$$

where V_{max} is the upper limit of measured visibility (50 km) and V_{rec} is the visibility recorded within the dust event record. DVR provides a numerical value for dust entrainment event intensity (from 0 to 50km) without the need to classify events into different types. The DVR data was presented as a cumulative total of those stations recording an event (rather than an average across stations) because, in our opinion this is the best way of illustrating the combined effects of the frequency and intensity of dust entrainment events. *McTainsh et al.* [1989] derived a linear relationship between dust storm frequency and spatial extent, suggesting the main controls on dust storms in Australia are climatic rather than local (soils or vegetation). High total DVR values therefore indicate widespread dust entrainment rather than a localized severe reduction in visibility.

2.2. Satellite Data

[14] The SeaWiFS sensor collects reflectance data in the visible spectrum, which can be related to CHL level. SeaWiFS also measures reflectance at 865 nm (a wavelength at which the ocean's reflectance is minimal) to derive the AOD. The over-ocean AOD is proportional to aerosol particle concentration from the sea surface to the top of the atmosphere and can be retrieved with an accuracy of 10% [*Gordon and Wang*, 1994; *Wang et al.*, 2000]. The AOD is mainly influenced by aerosols in the marine boundary layer (height: 0–1000 m), and scattering by particles in the size fraction below 10 μm in diameter [*Collins et al.*, 2000]. It is important to note that mineral dust, sea salt and non-sea-salt (nss) sulfate aerosols (e.g., from biogenic dimethylsulfide (DMS) emissions) can all contribute to the satellite registered AOD, albeit in different particle size ranges. Dust and sea-salt particles are mainly in the 1–2.5 micron range (coarse mode), with nss-sulfate, which in the remote SO is mainly derived from emissions of DMS, in the finer submicron range [*Gondwe et al.*, 2003]. This makes it difficult to unequivocally associate changes in AOD with dust loading in global data sets [*Cropp et al.*, 2005]. However, here we have examined the AOD record when we know that dust has been entrained and advected into the study region. In order to establish an approximate climatology for the study region, we analyzed monthly CHL and AOD data from the SeaWiFS sensor for the period September 1997 to August 2006. To investigate the dynamical changes during the study period, we also analyzed daily SeaWiFS data for the austral spring-summer months of 2002–2003.

2.3. Dust Transport Modeling

[15] The connection between individual dust storm events in southern Australia and resultant deposition over the adjacent ocean was investigated using the integrated wind erosion and dust transport model (CEMSYS) to simulate the daily deposition during November 2002 to February 2003. CEMSYS has been used for modeling several dust storms in Australia [*Lu and Shao*, 2001; *Shao and Leslie*, 1997] and was successfully validated using concurrent dust concentration data for a major dust storm event that moved northeast over the continent during October 2002, just prior to our period of interest [*McTainsh et al.*, 2005; *Shao et al.*, 2007]. CEMSYS is a process based model which couples an atmospheric submodel, a wind erosion submodel, and a dust deposition and transport submodel. These submodels are supported by a GIS database. The structure and details of the various submodels is outlined by *Shao and Leslie* [1997] and *Lu and Shao* [2001]. CEMSYS takes into account the atmospheric conditions (wind speed, rainfall and tempera-

Table 1. Summary of Land Surface Information Used in the CEMSYS Simulations

Parameter	Data Source
Aerodynamic roughness	Constant for bare soil, derived from vegetation height and LAI for vegetated surfaces [*Raupach*, 1994]
Zero-displacement height	Zero for bare soil, derived from vegetation height and LAI for vegetated surfaces [*McVicar et al.*, 1996]
Leaf Area Index	Derived from SeaWiFS normalized difference vegetation index data
Vegetation height	Adapted from *Australian Surveying and Land Information Group* [1990]
Soil particle-size distribution	Particle-size analysis of selected soil samples
Soil moisture	Soil moisture model integrated into CEMSYS

ture), soil conditions (soil texture and soil water) and surface vegetation.

[16] For this study, CEMSYS was run at 30 × 30 km resolution over Australia and the Southern Ocean for the simulation period. Atmospheric conditions used in the CEMSYS simulations for each day in the simulation period were obtained from HIRES, a High Resolution limited area atmospheric prediction model developed by *Leslie* [1998]. Land surface information required for the CEMSYS simulations is summarized in Table 1. It was assumed that vegetation cover was slowly varying and therefore constant for each month in the simulation. Vegetation cover for each month was estimated based on each month's Leaf Area Index (LAI). LAI values for each month were calculated from SeaWiFS normalized difference vegetation index (NDVI) data using the empirical relationships developed by *McVicar et al.* [1996]. Soil texture across the continent was divided up into 28 soil classes. Each soil class was characterized by a particle-size density function. The particle-size distributions of each soil class were considered to be unchanged during wind erosion events. Soil moisture varied considerably during the simulation period and was modeled accordingly within CEMSYS [*Shao et al.*, 1997].

2.4. Field Data

[17] Observations of sea surface chlorophyll *a*, fCO_2, temperature and salinity were carried out onboard the RSV Astrolabe on three return cruises between Hobart, Tasmania and Dumont D'Urville, Antarctica during the period October 2002 to March 2003. The sea surface continuous fCO_2 measurement technique has been previously described [*Metzl et al.*, 1999]. The net CO_2 flux (F) across the air-sea interface was determined from

$$F = ks\Delta fCO_2,$$

where *k*, the gas transfer velocity, was evaluated using the cubic wind speed relationship of *Wanninkhof and McGillis* [1999]; *s*, the solubility of CO_2 in seawater at the in situ temperature and salinity was calculated using the algorithm of *Weiss* [1974]. The interfacial fugacity gradient, ΔfCO_2, is the difference between fCO_2 in surface seawater ($fCO_{2\ sw}$) and in the atmosphere ($fCO_{2\ air}$):

$$\Delta f\,CO_2 = fCO_{2\,sw} - fCO_{2\,air}$$

The ΔfCO_2 sets the direction of CO_2 gas exchange (a negative value corresponds to drawdown) and is controlled by a combination of complex physical, chemical and biological processes in the ocean that determine the fCO_2 of seawater.

3. Results and Discussion

3.1. Dust Storm Observations

[18] A climatology of the annual total DVR at 111 long-term stations across Australia for the period 1960–2006 is shown in Figure 1. Years of high DVR almost always coincide with drought conditions in Australia. One of the highest annual total DVR in the 47 year time series was recorded during our study period with both 2002 and 2003 having total DVR > 40000. Figure 2 shows a comparison of monthly DVR for the study period together with the climatological mean monthly value. During the study period DVR was significantly higher than the long-term mean from September 2002 to March 2003, underscoring the consistently high dust storm activity. Peak monthly DVR was recorded on October 2002, with a slightly lower but significant peak in January 2003, which is not seen in the long-term record.

[19] The sum of the DVR values during October 2002 to February 2003 from all stations which recorded a dust event (including multiple daily DVR records when they occurred) was smoothed with a 3 day running mean and is shown in Figure 3a, together with Hovmoller plots of satellite derived AOD (Figure 3b) and CHL (Figure 3c) for the entire period in the study region. Significant dust transport during 2002 was directed to the northeast of the continent and not affecting our study region. Filled circles highlight those periods during which synoptic winds transported dust south over the SO.

[20] There is a clear temporal coherence between peaks in DVR and AOD in our study region for those dust storms advected south over the SO, particularly during early November 2002 (days 30–40), when elevated AOD was recorded as far as 53°S. This provides evidence that dust emission episodes on the Australian continent can significantly affect the optical characteristics of the atmosphere over the SO. Interestingly, there was little phytoplankton response associated with this event (Figure 3c), probably due to unfavorable ocean conditions (a deep mixed layer) at this time of the year.

[21] The continental dust storm activity during this period is summarized in Figure 4a where moderate to strong dust storms occurred along the eastern side of the continent. The synoptic meteorological conditions given in Figure 4b, indicate that strong northerly winds preceded an intense cyclonic system south of the continent. Figure 4c graphically illustrates the visibility reduction in the town of Griffith (34°S, 146°E) in southeast New South Wales, as the dust storm passed through.

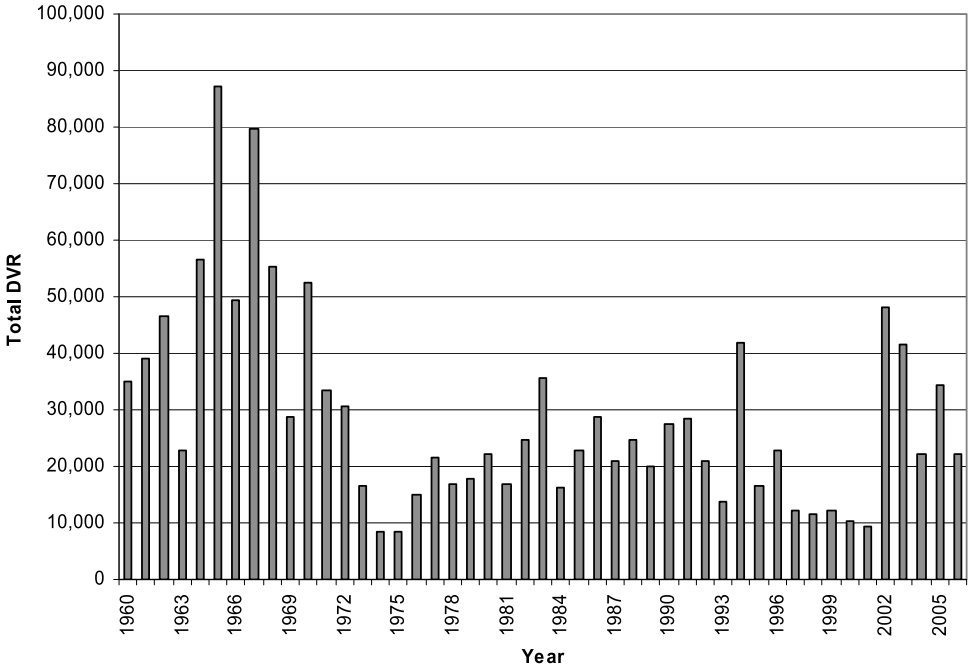

Figure 1. Annual total dust visibility reduction (DVR) across Australia at the 111 locations with long-term dust event records for the period 1960 to 2006.

3.2. Model Simulated Dust Deposition

[22] Except for the large event in late October which was transported to the northeast, several major dust plumes on the Australian continent were advected south and from west to east over the SO during the study period. We have chosen to illustrate the event that occurred during early November. The CEMSYS simulated time series of daily average total (wet + dry) deposition from 10–17 November (days 40–47) is shown in Figure 5. The dust plumes migrate across the study region on 11, 12, and 13 November which is clearly registered in the SeaWiFS AOD record (Figure 3b). The southerly extent of the simulated deposition highlights the long distance (to 60°S on 13 November) that Australian dust can be transported by prefrontal northerlies during the westerly passage of synoptic weather patterns.

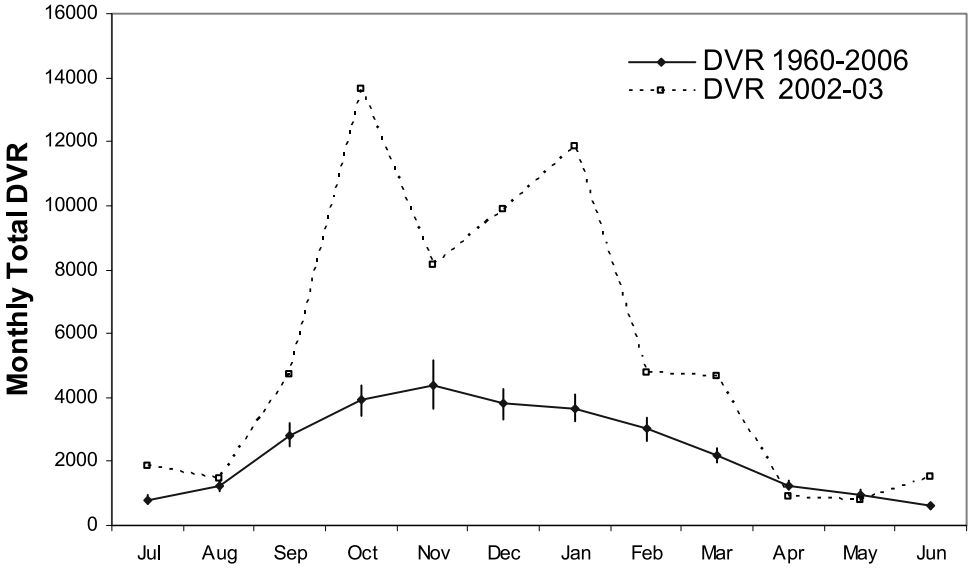

Figure 2. Monthly mean total DVR across Australia at 111 locations with long-term dust event records for the period 1960 to 2006 (with standard error) and monthly total DVR during the 2002–2003 study period.

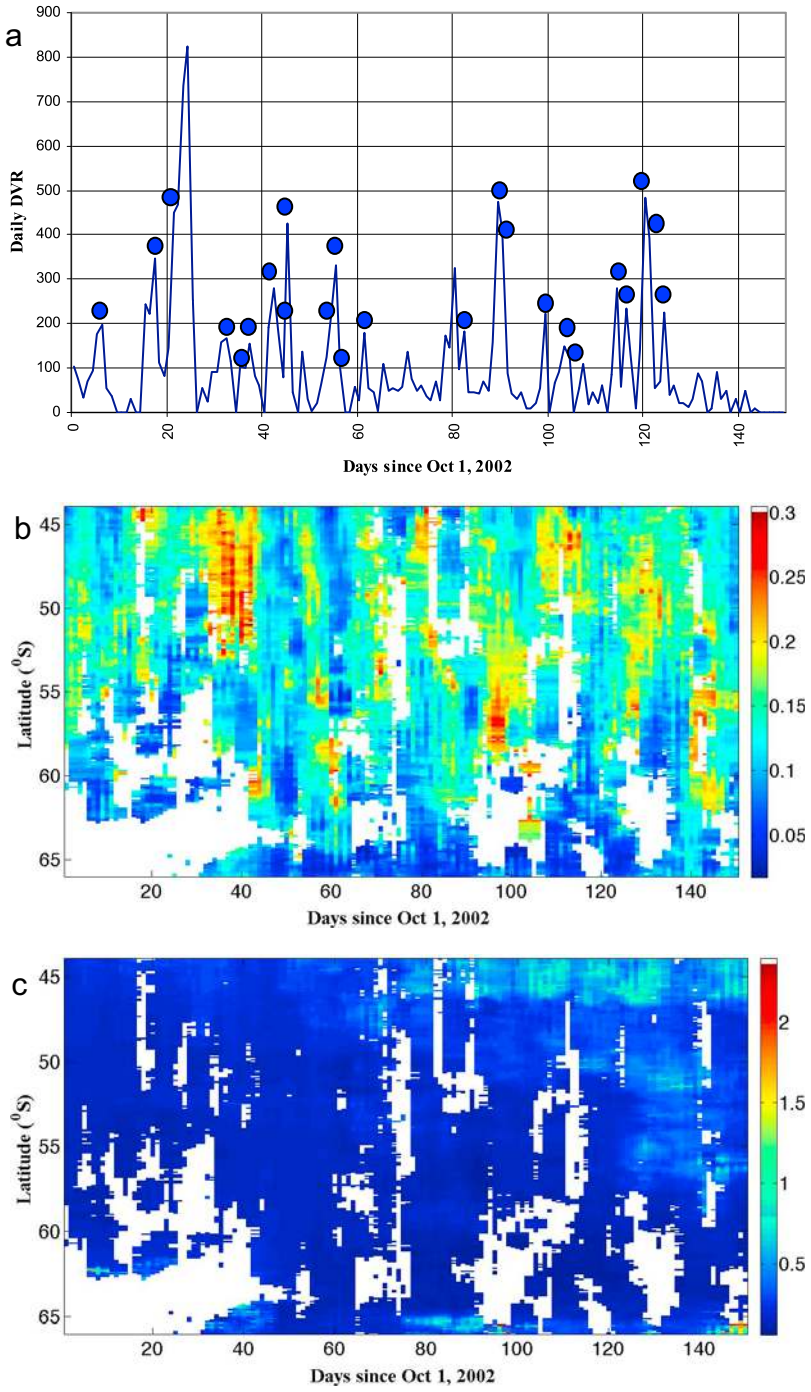

Figure 3. (a) Daily Dust Visibility Reduction from 1 October 2002 to 28 February 2003. Filled circles indicate those dust storm events where prevailing winds transported dust over the Southern Ocean (SO). Hovmoller plots of daily smoothed (b) SeaWiFS aerosol optical depth (AOD) and (c) SeaWiFS CHL (mg m^{-3}).

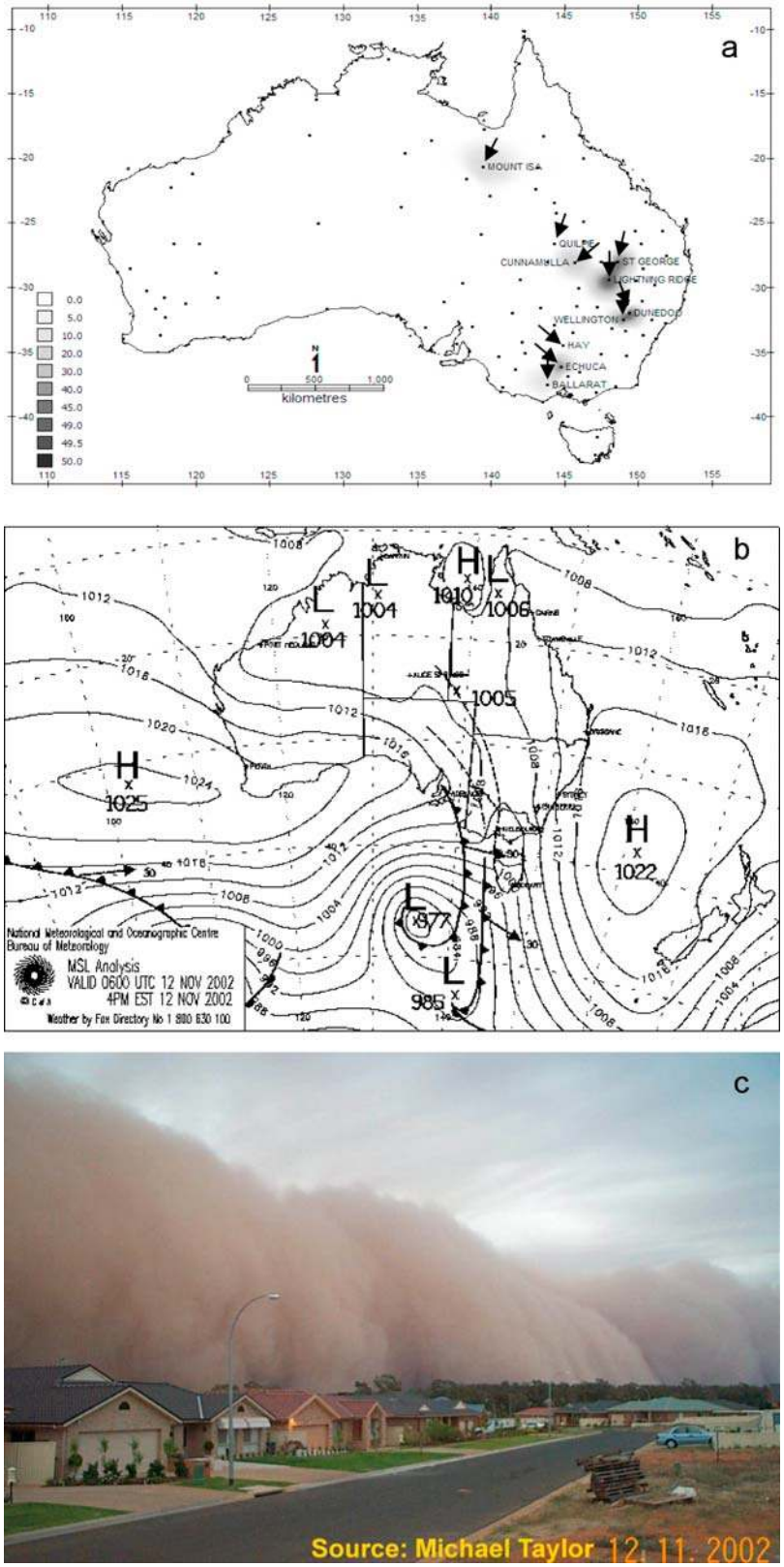

Figure 4. (a) Map of Australia showing dust events across the continent with wind direction arrows on 12 November 2002. Dust event intensity represented by DVR. (b) Synoptic meteorological chart. (c) Dust storm passing through Griffith, in southeast New South Wales.

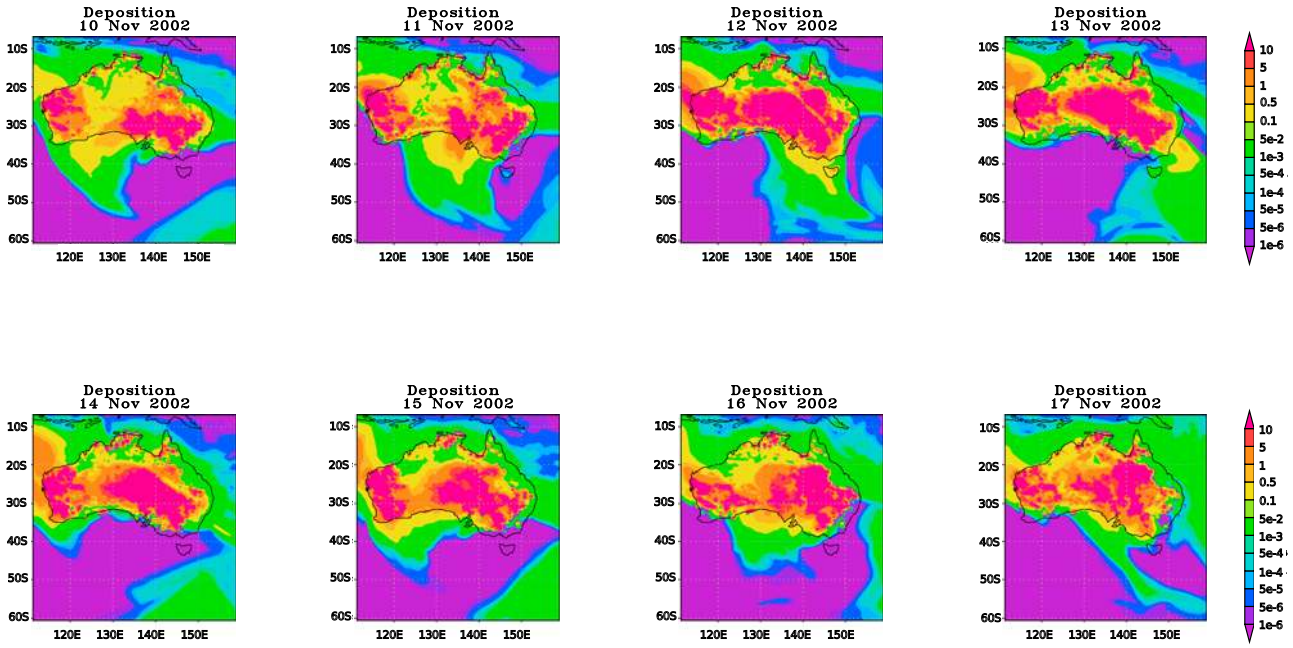

Figure 5. Simulated daily mean dust deposition over SO (μg m^{-2} s^{-1}) from CEMSYS model for the period 10–17 November 2002.

[23] Hovmoller plots of simulated dust loading and deposition for the entire time period are shown in Figures 6a and 6b. The simulated loading was high during mid-November and December and late January, periods corresponding to synoptic meteorological conditions which advected the dust south over the SO. Simulated deposition was high during the same periods. Both loading and deposition was highest in the northern sections but significant deposition was simulated as far as 55°S during December and again in late January. Notably, there was little loading or deposition simulated during February 2003, which was consistent with the DVR record of daily dust emission on the continent (Figure 3a).

3.3. Was 2002–2003 an Unusual Season?

[24] The DVR record confirms (Figure 2) that dust storm activity was certainly well above the norm throughout the study period, but did this translate to higher aerosol burden and deposition over the ocean? To ascertain the relative impact of the 2002–2003 dust storm season on the aerosol burden and CHL patterns of the adjacent SO, the 9 year archive of monthly SeaWiFS CHL and AOD was analyzed in 5 degree latitude bands for our study region. Figure 7 shows anomalies from the 9 year monthly means for the entire time series and confirms that positive CHL and AOD anomalies were registered in late 2002 in all but the most southerly latitude band. During early 2003, CHL displayed strong positive anomalies in the three bands covering 40°–55°S. Intriguingly, the positive CHL anomaly (~0.15 mg m^{-3}) recorded in the 50°–55°S band during 2002–2003 (Figure 7c) was the highest within the entire 9 year period, suggesting higher than normal primary productivity during our study period. The AOD anomalies were less pronounced, although moderately positive values were recorded during the spring of 2002, in the 40°–45°S and 45°–50°S bands.

[25] Although field data on CO_2 fugacity are sparse, *Breviere et al.* [2006] compared observations and ocean state in February 2003 with February 1997, and found significantly higher drawdown at latitudes south of 54°S during our study period (Figure 9a). As fCO_2 is controlled by a variety of physical factors in addition to enhanced biological activity, it is important to evaluate the relative impact of these other factors such as interannual variability in MLD, ocean temperature and surface wind speed. The observed MLD range during the summer of 2002–2003 (40–50 m) was similar to the climatological mean (Figure 9b). The mean monthly wind speed over the 50°–60°S band in February 2003, was about 10.1 m s^{-1} (ERS-2 and QuikSCAT MWF products) and also similar to the climatological mean [*Breviere et al.*, 2006]. The similarity in wind speeds and MLD between years suggests that changes in upper ocean mixing and gas exchange rates cannot explain the observed variability in surface fCO_2 during early 2003.

3.4. Chlorophyll Variability During the 2002–2003 Austral Summer

[26] The SeaWiFS record shows CHL increasing from day 100 in the 40°–45°S and 45°–50°S bands, but not until day 115 in the 50°–55°S and 55°–60°S bands (Figure 8). The season maximum in 40°–45°S, the region closest to the continent and therefore likely to respond earliest to dust deposition, was achieved in late January. In contrast, the maxima in more southerly bands were not achieved until February and March 2003. It is interesting to compare this trend with the 9 year mean climatology for CHL cycle also

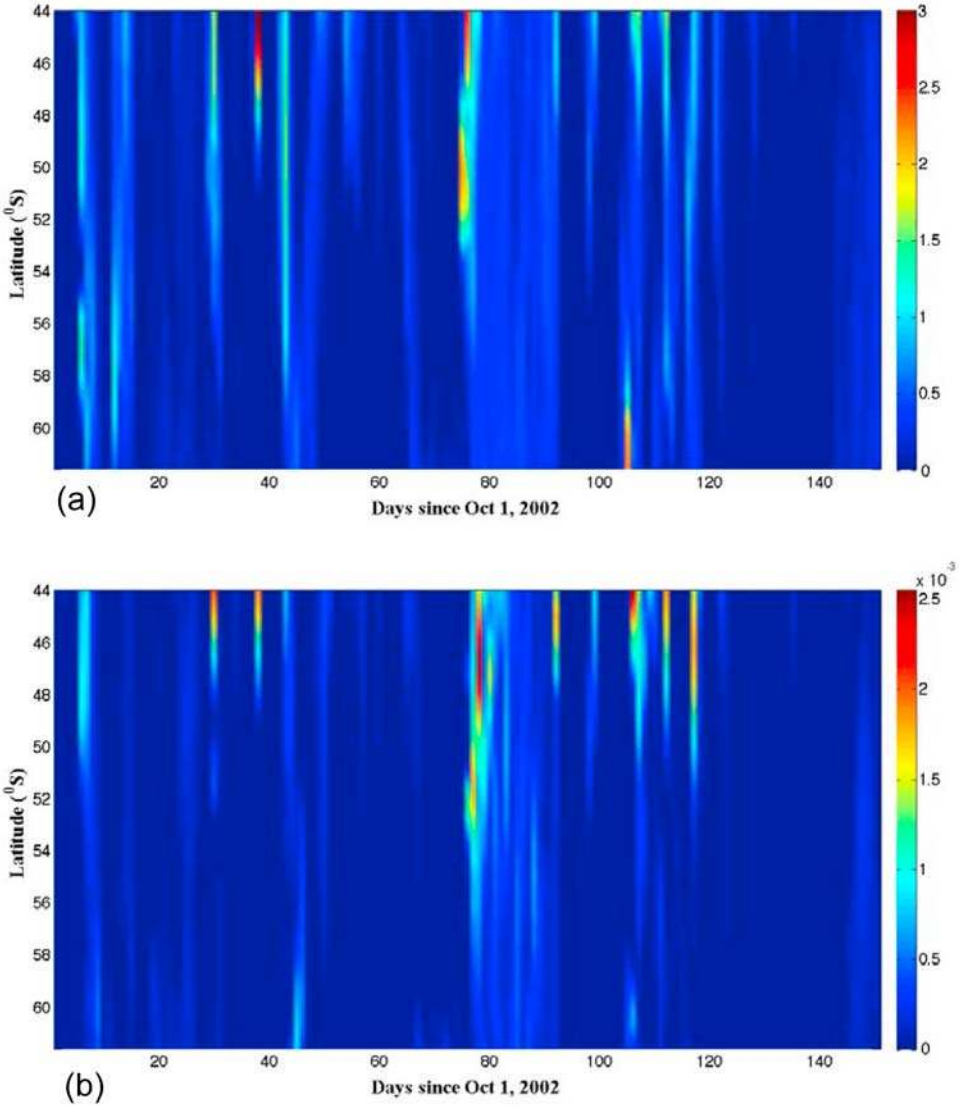

Figure 6. Hovmoller plots of CEMSYS simulated square-root-transformed (a) dust loading (mg m^{-2}) and (b) dust deposition (μg m^{-2} s^{-1}).

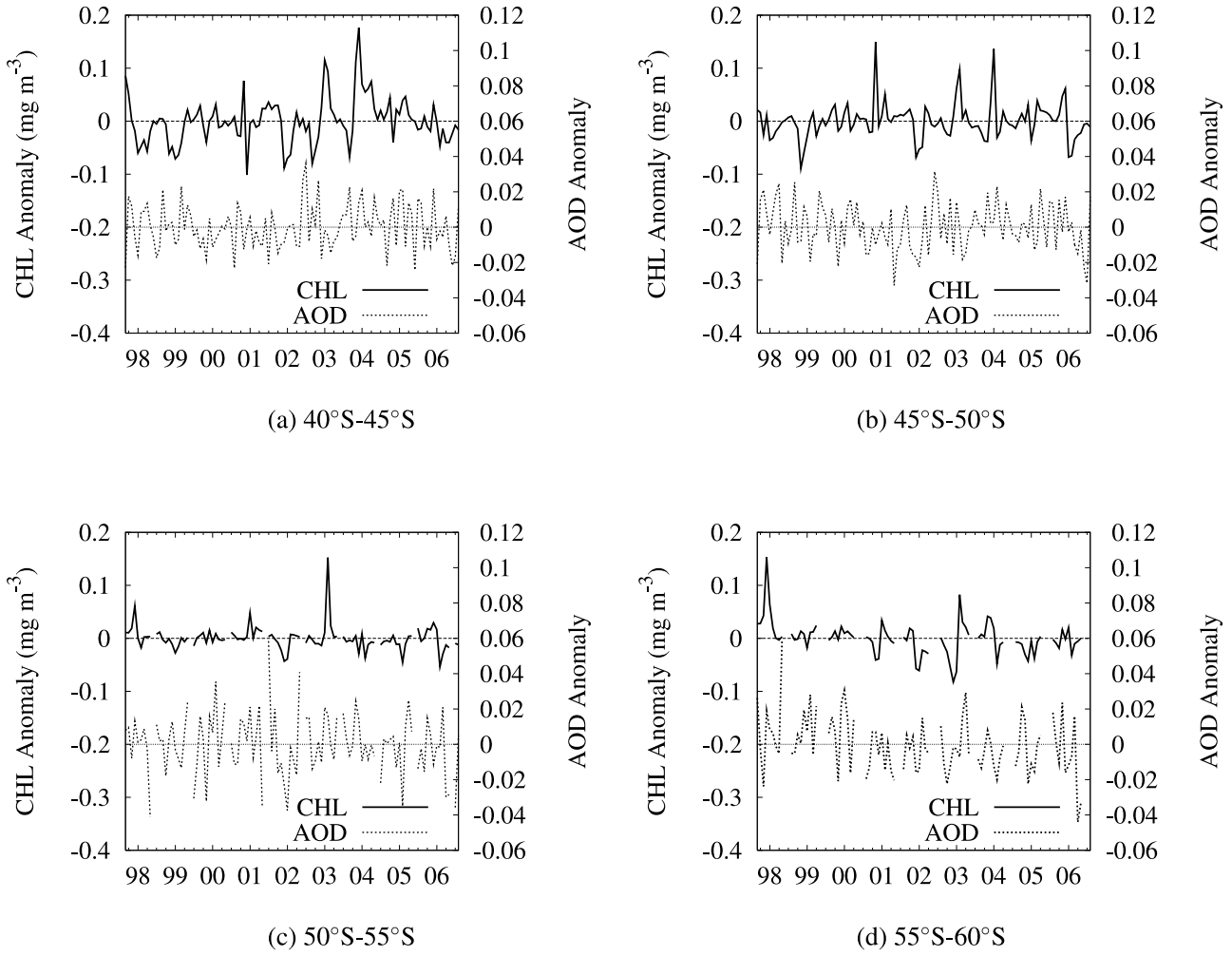

Figure 7. Deviations from the 9 year monthly mean for CHL and AOD in each 5 degree latitude band.

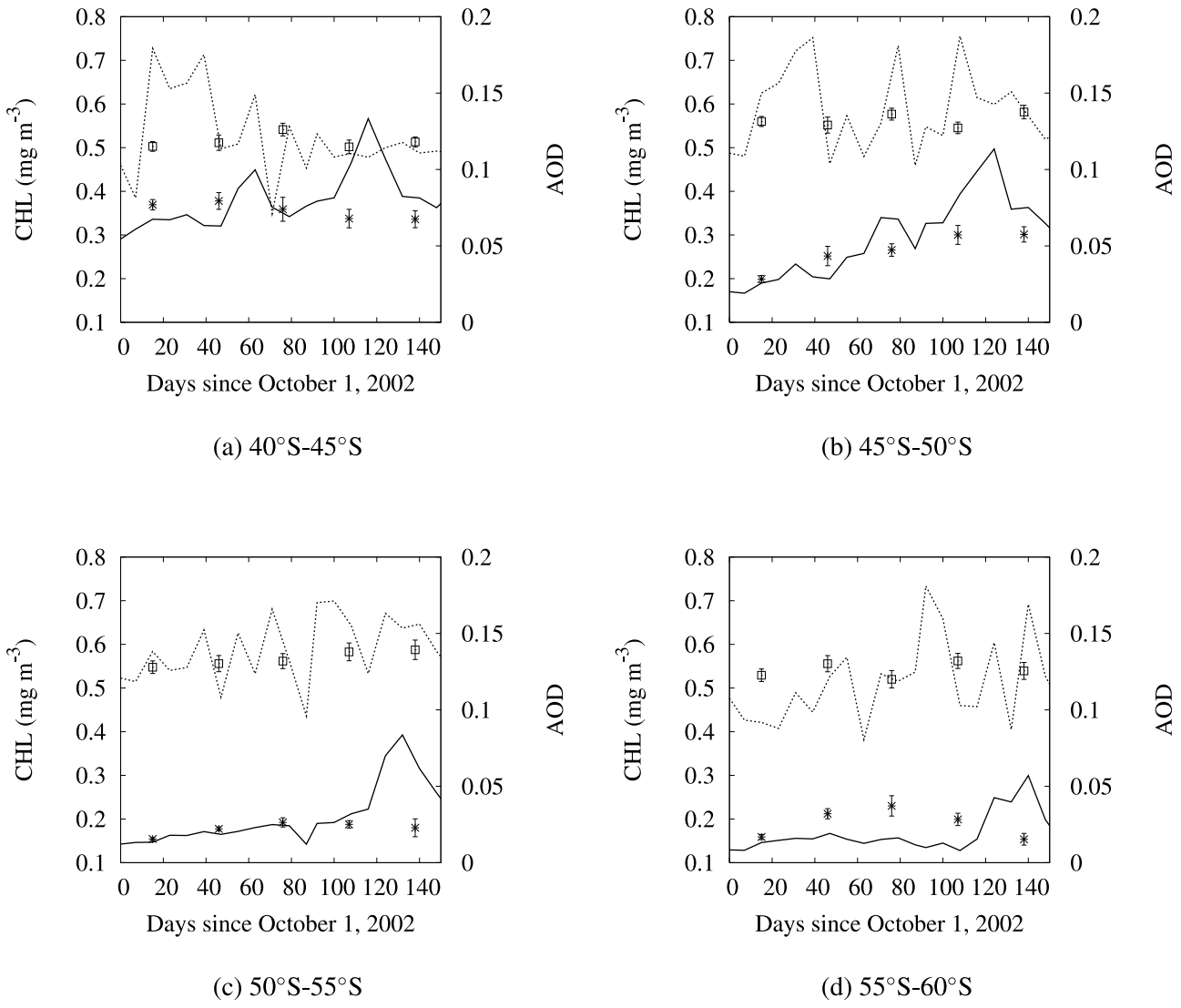

Figure 8. CHL and AOD time series from 1 October 2002, in 5 degree bands with 9 year climatological means overlaid (solid line, CHL; asterisks, CHL climatology; dotted line, AOD; boxes, AOD climatology, with standard deviations).

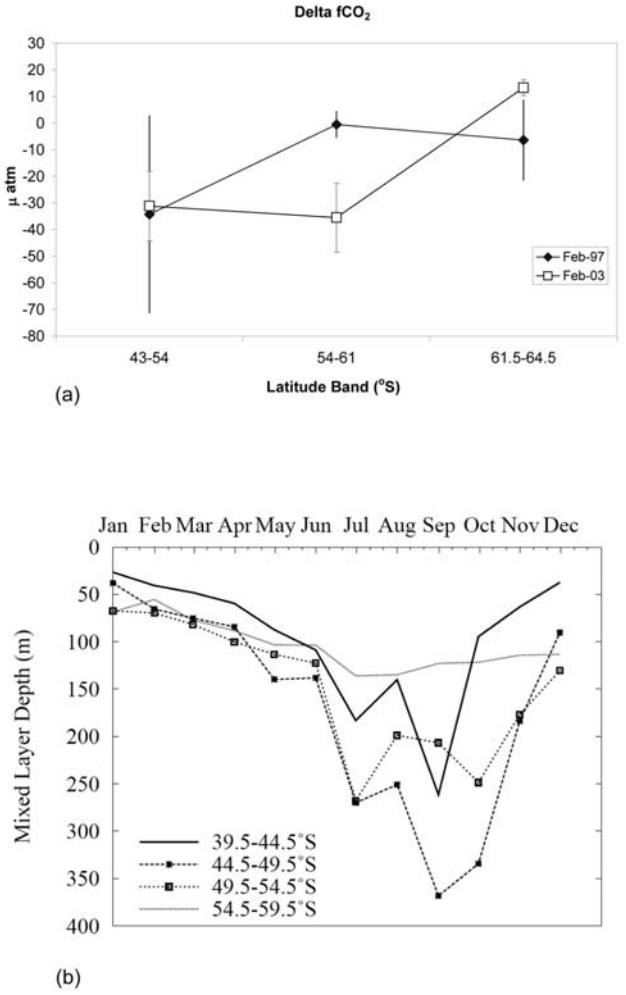

Figure 9. (a) CO_2 fugacity (μatm) in February 1997 and February 2003 from *Breviere et al.* [2006]. (b) Climatological mixed layer depths averaged in 5 degree bands in the study region [see *Conkright et al*., 2002].

given in Figure 8, where the maximum in all bands, except 45°–50°S, occurs late in spring or in summer, suggesting that the phenology of the phytoplankton bloom in 2002–2003 was unusual, with both the timing occurring later in the season and the magnitude being higher than the climatological maximum. The space-time variation in chlorophyll measured along the cruise tracks (Figure 10b) is generally consistent with the satellite record (Figure 3c), notwithstanding the problems in directly comparing Figures 3c and 10b, due to the latter being a linear interpolation in time between the dates of the cruise transects, which were more than 30 days apart.

[27] The climatological seasonality in surface chlorophyll is thought to be mainly due to change in the MLD, which in the SO varies dramatically between summer and winter [*de Boyer-Montegut et al.*, 2004]. In our study region, the MLD varies from almost 400 m in winter to less than 30 m in January [*Boyer and Levitus*, 1994]. In all seasons except summer, the deep mixed layer imposes a severe light limitation on phytoplankton growth [*Boyd*, 2002]. During January and February, the MLD decreases (Figure 9b) and light limitation is relieved, with phytoplankton growth then only limited by availability of Fe, as macronutrients are replete throughout the year [*Boyd*, 2002]. The Fe limitation hypothesis in the SO has been confirmed by in situ iron fertilization experiments, for example, SOIREE and SOFex [*Boyd and Law*, 2001; *Coale et al.*, 2004], but algal response to Fe addition is complex, displaying both regional and taxonomic variability.

3.5. CO_2 Fugacity Data

[28] Figures 10a and 10b show Hovmoller diagrams of the space-time interpolated ΔfCO_2 and surface chlorophyll data collected along cruise tracks (dotted lines) between Hobart (about 148°E) and Dumont D'Urville at 140°E on the Antarctic continent. We note that the time interval between successive sampling at the same location was from 25 to 30 days leading to the possibility that some events were missed or undersampled. Figure 10a indicates that CO_2 drawdown in the northern section of the study region commenced in November and was high from late December through to March. Between late January (~day 115) and mid-February (~day 140) there was also a significant increase in drawdown between 50°S and 60°S, that persisted through early March, and coincided with the timing of peak biomass (CHL) in 50°–60°S (Figures 8c and 8d). It is notable that CHL concentrations achieved at this latitude during the study period were the highest in the 9 year record (Figure 7c). This suggests the possibility that Fe limitation was relieved during this period, presumably by dust-derived Fe deposition. It is also notable that peak CHL in all latitude bands (except 40°–45°S) was not achieved until February (Figure 8). The MLD climatology (Figure 9b) indicates that minimum annual MLD occurs during January–February, relieving light limitation as a factor in the phytoplankton response.

3.6. Factors Affecting the Bioavailability of Fe

[29] A broad range of physical, chemical and biological factors can affect dust-derived Fe solubility in both the marine atmosphere and upper ocean [*Baker and Croot*, 2010]. Of particular relevance to our SO region, which is recognized to be a major source of biogenic DMS during the austral summer [*Kettle and Andreae*, 2000], is a possible interaction between dust-borne Fe and acidic aerosols. The production of DMS by phytoplankton causes an increase in the acidity of overlying marine aerosols and the possibility of in-cloud dissolution of dust-associated Fe(III) [*Zhu et al.*, 1992]. Evidence for this was presented by *Zhuang et al.* [1992] who reported that over 50% of the total Fe present in remote marine aerosols is in the soluble Fe (II) form, with the Fe (II) fraction amplified significantly during long-range transport, and then readily bioavailable to phytoplankton. The photoreduction reaction that produces Fe (II) in aerosols also produces the hydroxyl (OH) radical, which is required for the oxidation of gaseous DMS to MSA, thus providing a feedback on Fe(III) dissolution [*Zhuang et al.*, 2003].

[30] More recently, laboratory experiments have provided evidence for a direct link between DMS oxidation by-products and aerosol Fe bioavailability. *Johansen and Key*

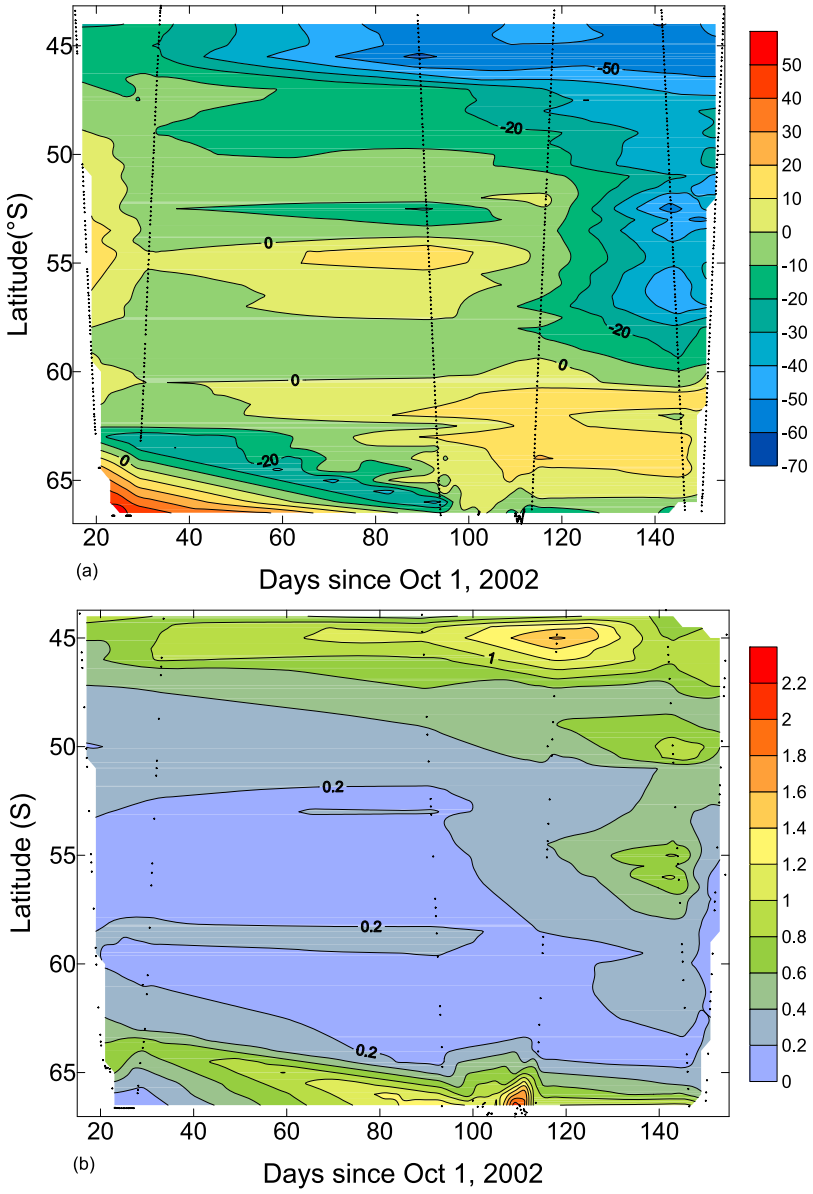

Figure 10. (a) Sea-air gradient in fCO_2 along cruise tracks (dotted lines) and interpolated over time and space; negative values indicate drawdown. (b) CHL along cruise tracks and interpolated over space and time (mg m^{-3}).

[2006] and *Key et al.* [2008] have shown that dissolution of ferrihydrite, a surrogate iron(oxy)hydroxide phase found in atmospheric waters, is enhanced in the presence of methanesulfinic acid (MSIA) (a DMS oxidation product), in experiments with aqueous suspensions that simulate marine aerosol particles.

[31] A multidecadal times series of atmospheric MSA (which is solely derived from DMS) at Cape Grim is shown in Figure 11a. Although there is interannual variability in the magnitude of the MSA peak, the strong seasonality and early January (days 92–100) timing of the MSA maximum is remarkably robust, with peak values in the range 1.5–3.5 nmol m^{-3}. The weekly time series of atmospheric MSA during our study period (Figure 11b) shows that the highest seasonal values (2.6 nmol m^{-3}) were achieved during January with moderately high values (>0.5 nmol m^{-3}) maintained through March. The impacts on aerosol acidity and thus potentially Fe solubility would have been maximal during January when dust was being advected south and ocean conditions were most favorable to phytoplankton growth (Figures 3a and 6b).

[32] Another intriguing possibility affecting Fe solubility was raised by *Bowie et al.* [2009], who measured Fe dissolution values in the range 0.2%–2.5% for samples in the SAZ during January 2007, but a significantly higher value of 17.7%, in a sample that may have included particles emitted from forest fires burning at the time. Higher Fe solubility in biomass combustion particles has been sug-

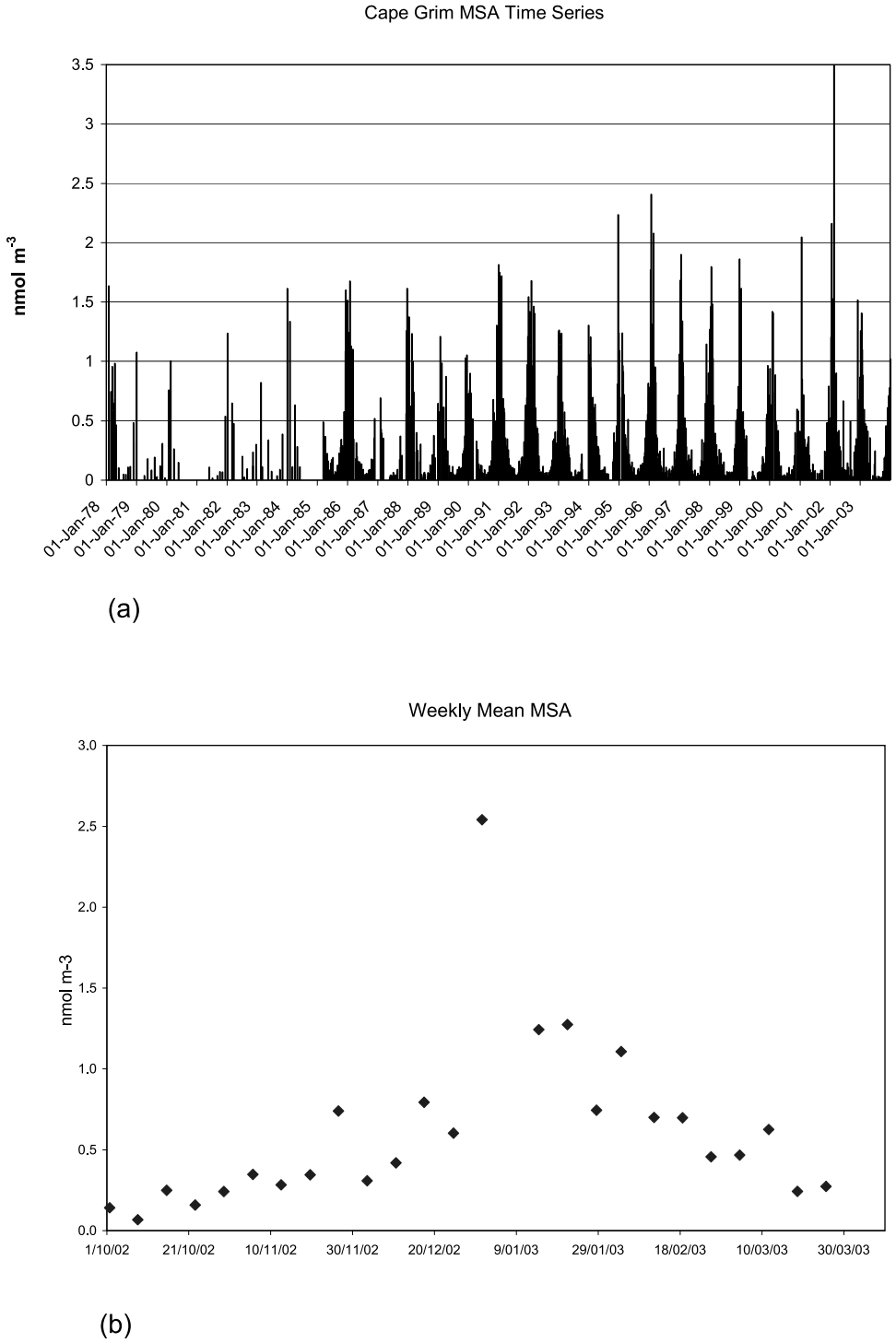

Figure 11. (a) Long-term methanesulfonic acid (MSA) time series measured at Cape Grim (Tasmania) 1978–2003. (b) MSA (nmol m^{-3}) at Cape Grim from October 2002 to March 2003.

gested in former studies [*Guieu et al.*, 2005], and there were extensive forest fires in Canberra and southern NSW during the second half of January 2003 [*Chen and McAneney*, 2004].

4. Conclusions

[33] We have presented various data indicators of ocean and atmospheric state to explore the connection between the very active Australian dust storm season of 2002–2003, and the biogeochemical response of the adjacent SO. Unfortunately, we do not have field data on dissolved Fe concentrations during the study period, which would strengthen the evidence for a dust-driven biological response. However, continental observations of DVR and dust transport model simulations suggest the delivery of dust to the adjacent SO to have been significant, albeit episodic. The contemporaneous satellite record indicates the dust loading affected the aerosol climate, but because of the various possible influences on AOD it is difficult to be unequivocal in this regard. Major dust storm events that were advected south in late October, early November and January had a clear affect on AOD values in the 40°–45°S and 45°–50°S bands, closest to the Australian continent, suggesting a strong coherence between the optical characteristics of the SO atmosphere and dust loading.

[34] Satellite and field data on surface chlorophyll indicate a significant biological response, which was unusually strong south of 50°S. With the exception of the 40°–45°S band, the SeaWiFS CHL record shows a similar temporal trend in all latitude bands, with CHL increasing from day 100 in the 40°–50°S region, but not until day 115 in the 50°–60°S region (Figure 8). Except for the northern most band, peak CHL was achieved after day 120 (29 January 2003), which was unusual when compared with the available 9 year CHL climatology. Field data show this was associated with a strong CO_2 drawdown, commencing at day 120, which does not seem to have been due to atypical mixed layer depth or winds. Dust storm activity was strong in December and late January but started to subside in February.

[35] The apparent time lag between dust deposition to the ocean in late January and the biological response in the more southerly zones in February–March is intriguing. Such a lag between iron fertilization and peak biomass has been seen in artificial fertilization experiments where high CHL levels were recorded for some time after fertilization, up to four weeks or more [*Coale et al.*, 2004]. It is also possible that the algal response in these more southerly zones was unrelated to dust deposition; however, a convincing alternate explanation for the enhanced biological activity is not readily available from the data. A possible alternate hypothesis is that macronutrients and Fe have been advected horizontally into the 50°–60°S region either from subtropical waters to the north [*Bowie et al.*, 2009; *Sedwick et al.*, 2008] or from upwelling of nutrient-rich Upper Circumpolar Deep Water (UCDW) further south [*Pollard et al.*, 2006]. UCDW shoals as it upwells to the south, rising steeply near the subantarctic front (around 50°S) and continues to rise, outcropping south of the Polar Front which is between 55° and 60°S in our region. UCDW is then entrained in the surface Ekman layer, and moves toward the north, forming Antarctic Intermediate Water, when it downwells beneath the warmer Subantarctic Mode Water [*Hoppema et al.*, 2003].

[36] Our results provide strong circumstantial evidence for a coupling between dust deposition, Fe delivery and biogeochemical response in the Australian sector of the SO which merits further ongoing investigation. This is especially important as global climate model projections suggest that Australia will experience negative precipitation anomalies in the future, with a possible increase in drought and dust storm frequency and severity. Although our data document a very active dust storm season, they raise the possibility that future enhanced delivery of Australian dust and associated Fe to the SO may have significant impacts on the regional SO carbon sink, and should not be ignored in projections of regional oceanic carbon budgets.

[37] **Acknowledgments.** Access to the CEMSYS model was generously provided by Yaping Shao (University of Cologne). The dust work (GMcT) was supported by an Australian Research Council grant, and data analyses were performed by Kenn Tews. Grant support from the Australian Antarctic Division is gratefully acknowledged. We are grateful to two anonymous reviewers whose insightful comments improved this manuscript.

References

Abelmann, A., R. Gersonde, G. Cortese, G. Kuhn, and V. Smetacek (2006), Extensive phytoplankton blooms in the Atlantic sector of the glacial Southern Ocean, *Paleoceanography*, *21*, PA1013, doi:10.1029/2005PA001199.

Australian Surveying and Land Information Group (1990), Atlas of Australian Resources: Vegetation, Austr. Gov. Publ. Serv., Canberra, ACT, Australia.

Ayers, G. P., J. P. Ivey, and R. W. Gillett (1991), Coherence between seasonal cycles of dimethylsulphide, methansulponate and sulphate in marine air, *Nature*, *349*, 404–406, doi:10.1038/349404a0.

Baker, A. R., and P. L. Croot (2010), Atmospheric and marine controls on aerosol iron solubility in seawater, *Mar. Chem.*, doi:10.1016/j.marchem.2008.09.003, in press.

Bakker, D. C. E., A. J. Watson, and C. S. Law (2001), Southern Ocean iron enrichment promotes inorganic carbon drawdown, *Deep Sea Res., Part II*, *48*, 2483–2507, doi:10.1016/S0967-0645(01)00005-4.

Bakker, D. C. E., Y. Bozec, P. D. Nightingale, L. Goldson, M. J. Messias, H. J. W. de Baar, M. Liddicoat, I. Skjelvan, V. Strass, and A. J. Watson (2005), Iron and mixing affect biological carbon uptake in SOIREE and EisenEx, two Southern Ocean iron fertilisation experiments, *Deep Sea Res., Part I*, *52*, 1001–1019, doi:10.1016/j.dsr.2004.11.015.

Behra, P., and L. Sigg (1990), Evidence for redox cycling of iron in atmospheric water droplets, *Nature*, *344*, 419–421, doi:10.1038/344419a0.

Bishop, J. K. B., R. E. Davis, and J. T. Sherman (2002), Robotic observations of dust storm enhancement of carbon biomass in the North Pacific, *Science*, *298*, 817–821, doi:10.1126/science.1074961.

Bonnet, S., and C. Guieu (2004), Dissolution of atmospheric iron in seawater, *Geophys. Res. Lett.*, *31*, L03303, doi:10.1029/2003GL018423.

Bowie, A. R., D. Lannuzel, T. A. Remenyi, T. Wagener, P. J. Lam, P. W. Boyd, C. Guieu, A. T. Townsend, and T. W. Trull (2009), Biogeochemical iron budgets of the Southern Ocean south of Australia: Decoupling of iron and nutrient cycles in the subantarctic zone by the summertime supply, *Global Biogeochem. Cycles*, *23*, GB4034, doi:10.1029/2009GB003500.

Boyd, P. W. (2002), Environmental factors controlling phytoplankton processes in the Southern Ocean, *J. Phycol.*, *38*, 844–861, doi:10.1046/j.1529-8817.2002.t01-1-01203.x.

Boyd, P. W., and C. S. Law (2001), The Southern Ocean Iron Release Experiment (SOIREE): Introduction and summary, *Deep Sea Res., Part II*, *48*, 2425–2438, doi:10.1016/S0967-0645(01)00002-9.

Boyd, P. W., and D. Mackie (2008), Comment on the Southern Ocean biological response to aeolian iron deposition, *Science*, *319*, 159, doi:10.1126/science.1149884.

Boyd, P. W., G. McTainsh, V. Sherlock, K. Richardson, S. Nichol, M. Ellwood, and R. Frew (2004), Episodic enhancement of phytoplankton stocks in New Zealand subantarctic waters: Contribution of atmospheric and oceanic iron supply, *Global Biogeochem. Cycles*, *18*, GB1029, doi:10.1029/2002GB002020.

Boyd, P. W., D. S. Mackie, and K. A. Hunter (2010), Aerosol iron deposition to the surface ocean: Modes of iron supply and biological responses, *Mar. Chem.*, doi:10.1016/j.marchem.2009.01.008, in press.

Boyer, T. P., and S. Levitus (1994), Quality control and processing of historical temperature, salinity and oxygen data, *NOAA Tech. Rep. NESDIS 81*, 65 pp.

Breviere, E., N. Metzl, A. Poisson, and B. Tilbrook (2006), Changes of the oceanic CO_2 sink in the eastern Indian sector of the Southern Ocean, *Tellus, Ser. B*, *58*, 438–446, doi:10.1111/j.1600-0889.2006.00220.x.

Broecker, W. S., and G. M. Henderson (1998), The sequence of events surrounding Termination II and their implications for the cause of glacial-interglacial CO_2 changes, *Paleoceanography*, *13*, 352–364, doi:10.1029/98PA00920.

Cassar, N., M. L. Bender, B. A. Barnett, S. Fan, W. J. Moxim, H. Levy, and B. Tilbrook (2007), The Southern Ocean biological response to Aeolian iron deposition, *Science*, *317*, 1067–1070, doi:10.1126/science.1144602.

Cassar, N., M. L. Bender, B. A. Barnett, S. M. Fan, W. J. Moxim, H. Levy, and B. Tilbrook (2008), Response to comment on "The Southern Ocean biological response to aeolian iron deposition," *Science*, *319*, 159, doi:10.1126/science.1150011.

Chen, K., and J. McAneney (2004), Quantifying bushfire penetration into urban areas in Australia, *Geophys. Res. Lett.*, *31*, L12212, doi:10.1029/2004GL020244.

Coale, K. H., et al. (2004), Southern ocean iron enrichment experiment: Carbon cycling in high- and low-Si waters, *Science*, *304*, 408–414, doi:10.1126/science.1089778.

Collins, D. R., et al. (2000), In situ aerosol-size distributions and clear-column radiative closure during ACE-2, *Tellus, Ser. B*, *52*, 498–525.

Conkright, M. E., H. E. Garcia, T. D. O'Brien, R. A. Locarnini, T. P. Boyer, C. Stephens, and J. I. Antonov (2002), *World Ocean Atlas 2001*, *NOAA Atlas NESDIS*, vol. 52, 392 pp., NOAA, Silver Spring, Md.

Cropp, R. A., A. J. Gabric, G. H. McTainsh, R. D. Braddock, and N. Tindale (2005), Coupling between ocean biota and atmospheric aerosols: Dust, dimethylsulphide, or artifact?, *Global Biogeochem. Cycles*, *19*, GB4002, doi:10.1029/2004GB002436.

Crosta, X., A. Shemesh, J. Etourneau, R. Yam, I. Billy, and J. J. Pichon (2005), Nutrient cycling in the Indian sector of the Southern Ocean over the last 50,000 years, *Global Biogeochem. Cycles*, *19*, GB3007, doi:10.1029/2004GB002344.

de Boyer-Montegut, C., G. Madec, A. S. Fischer, A. Lazar, and D. Iudicone (2004), Mixed layer depth over the global ocean: An examination of profile data and a profile-based climatology, *J. Geophys. Res.*, *109*, C12003, doi:10.1029/2004JC002378.

Edwards, R., and P. Sedwick (2001), Iron in East Antarctic snow: Implications for atmospheric iron deposition and algal production in Antarctic waters, *Geophys. Res. Lett.*, *28*, 3907–3910, doi:10.1029/2001GL012867.

Edwards, R., P. N. Sedwick, V. Morgan, C. F. Boutron, and S. Hong (1998), Iron in ice cores from Law Dome, East Antarctica: Implications for past deposition of aerosol iron, *Ann. Glaciol.*, *27*, 365–370.

Edwards, R., P. Sedwick, V. Morgan, and C. Boutron (2006), Iron in ice cores from Law Dome: A record of atmospheric iron deposition for maritime East Antarctica during the Holocene and Last Glacial Maximum, *Geochem. Geophys. Geosyst.*, *7*, Q12Q01, doi:10.1029/2006GC001307.

Gabric, A. J., R. Cropp, G. P. Ayers, G. McTainsh, and R. Braddock (2002), Coupling between cycles of phytoplankton biomass and aerosol optical depth as derived from SeaWiFS time series in the subantarctic Southern Ocean, *Geophys. Res. Lett.*, *29*(7), 1112, doi:10.1029/2001GL013545.

Gervais, F., U. Riebesell, and M. Y. Gorbunov (2002), Changes in primary productivity and chlorophyll a in response to iron fertilization in the Southern Polar Frontal Zone, *Limnol. Oceanogr.*, *47*, 1324–1335.

Gingele, F. X., and P. De Deckker (2005), Late quaternary fluctuations of palaeoproductivity in the Murray canyons area, South Australian continental margin, Palaeogeogr. *Palaeoclimatol. Palaeoecol.*, *220*, 361–373, doi:10.1016/j.palaeo.2005.01.012.

Gondwe, M., M. Krol, W. Gieskes, W. Klaassen, and H. de Baar (2003), The contribution of ocean-leaving DMS to the global atmospheric burdens of DMS, MSA, SO_2, and NSS $SO_4^=$, *Global Biogeochem. Cycles*, *17*(2), 1056, doi:10.1029/2002GB001937.

Gordon, H. R., and M. Wang (1994), Retrieval of water-leaving radiance and aerosol optical thickness over the oceans with SeaWiFS: A preliminary algorithm, *Appl. Opt.*, *33*, 443–452, doi:10.1364/AO.33.000443.

Guieu, C., S. Bonnet, T. Wagener, and M. D. Loÿe-Pilot (2005), Biomass burning as a source of dissolved iron to the open ocean?, *Geophys. Res. Lett.*, *32*, L19608, doi:10.1029/2005GL022962.

Hoppema, M., H. J. W. de Baar, E. Fahrbach, H. H. Hellmer, and B. Klein (2003), Substantial advective iron loss diminishes phytoplankton production in the Antarctic Zone, *Global Biogeochem. Cycles*, *17*(1), 1025, doi:10.1029/2002GB001957.

Hsu, S.-C., et al. (2010), Sources, solubility, and dry deposition of aerosol trace elements over the East China Sea, *Mar. Chem.*, in press.

Jickells, T. D., and L. Spokes (2001), Atmosphereic iron inputs to the oceans, in *The Biogeochemistry of Iron in Seawater*, edited by D. R. Turner and K. Hunter, pp. 85–122, John Wiley, New York.

Jickells, T. D., et al. (2005), Global iron connections between desert dust, ocean biogeochemistry, and climate, *Science*, *308*, 67–71, doi:10.1126/science.1105959.

Johansen, A. M., and J. M. Key (2006), Photoreductive dissolution of ferrihydrite by methanesulfinic acid: Evidence of a direct link between dimethylsulfide and iron-bioavailability, *Geophys. Res. Lett.*, *33*, L14818, doi:10.1029/2006GL026010.

Johnston, T. C., and R. B. Alley (2006), Possible role for dust or other northern forcing of ice-age carbon dioxide changes, *Quat. Sci. Rev.*, *25*, 3198–3206, doi:10.1016/j.quascirev.2006.10.003.

Kettle, A. J., and M. O. Andreae (2000), Flux of dimethylsulfide from the oceans: A comparison of updated data sets and flux models, *J. Geophys. Res.*, *105*, 26,793–26,808, doi:10.1029/2000JD900252.

Key, J. M., N. Paulk, and A. M. Johansen (2008), Photochemistry of iron in simulated crustal aerosols with dimethyl sulfide oxidation products, *Environ. Sci. Technol.*, *42*, 133–139, doi:10.1021/es071469y.

Kohfeld, K. E., C. Le Quere, S. P. Harrison, and R. F. Anderson (2005), Role of marine biology in glacial-interglacial CO_2 cycles, *Science*, *308*, 74–78, doi:10.1126/science.1105375.

Leslie, L. (1998), Weather forecasting models, in *Climate Prediction for Agricultural and Re-source Management*, edited by R. Munro and L. Leslie, pp. 103–116, Bur. of Resour. Sci., Canberra, ACT, Australia.

Lu, H., and Y. P. Shao (2001), Toward quantitative prediction of dust storms: An integrated wind erosion modelling system and its applications, *Environ. Model. Softw.*, *16*, 233–249, doi:10.1016/S1364-8152(00)00083-9.

Mackie, D. S., P. W. Boyd, G. H. McTainsh, N. W. Tindale, T. K. Westberry, and K. A. Hunter (2008), Biogeochemistry of iron in Australian dust: From eolian uplift to marine uptake, *Geochem. Geophys. Geosyst.*, *9*, Q03Q08, doi:10.1029/2007GC001813.

Mahowald, N., K. Kohfeld, M. Hansson, Y. Balkanski, S. P. Harrison, I. C. Prentice, M. Schulz, and H. Rodhe (1999), Dust sources and deposition during the last glacial maximum and current climate: A comparison of model results with paleodata from ice cores and marine sediments, *J. Geophys. Res.*, *104*(D13), 15,895–15,916, doi:10.1029/1999JD900084.

Marinov, I., A. Gnanadesikan, J. R. Toggweiler, and J. L. Sarmiento (2006), The Southern Ocean biogeochemical divide, *Nature*, *441*, 964–967, doi:10.1038/nature04883.

McGowan, H. A., G. H. McTainsh, P. Zawar-Reza, and A. Sturman (2000), Identifying regional dust transport pathways: Application of kinematic trajectory modelling to a trans-Tasman case, *Earth Surf. Process. Landforms*, *25*, 633–647, doi:10.1002/1096-9837(200006)25:6<633::AID-ESP102>3.0.CO;2-J.

McTainsh, G. H., and J. F. Leys (1993), Wind erosion, in *Land Degradation Processes in Australia*, edited by G. H. McTainsh and W. C. Boughton, chap. 7, pp. 188–233, Longman-Cheshire, Melbourne, Vic., Australia.

McTainsh, G. H., R. Burgess, and J. R. Pitblado (1989), Aridity, drought and dust storms in Australia (1960–84), *J. Arid Environ.*, *16*, 11–22.

McTainsh, G. H., A. W. Lynch, and E. K. Tews (1998), Climatic controls upon dust storm occurrence in eastern Australia, *J. Arid Environ.*, *39*, 457–466, doi:10.1006/jare.1997.0373.

McTainsh, G., Y. C. Chan, H. McGowan, J. Leys, and K. Tews (2005), The 23rd October 2002 dust storm in eastern Australia: Characteristics and meteorological conditions, *Atmos. Environ.*, *39*, 1227–1236, doi:10.1016/j.atmosenv.2004.10.016.

McVicar, T., J. Walker, D. Jupp, L. Pierce, G. Byrne, and R. Dallwitz (1996), Relating AVHRR vegetation indices to in situ measurements of leaf area index, CSIRO Div. of Water Resour., Canberra, ACT, Australia.

Meskhidze, N., W. L. Chameides, A. Nenes, and G. Chen (2003), Iron mobilization in mineral dust: Can anthropogenic SO_2 emissions affect ocean productivity?, *Geophys. Res. Lett.*, *30*(21), 2085, doi:10.1029/2003GL018035.

Metzl, N., B. Tilbrook, and A. Poisson (1999), The annual fCO_2 cycle and the air-sea CO_2 flux in the sub-Antarctic Ocean, *Tellus, Ser. B*, *51*, 849–861, doi:10.1034/j.1600-0889.1999.t01-3-00008.x.

Michard, G. (2008), Can we explain atmospheric carbon dioxide oscillations during the past 400,000 years?, *C. R. Geosci.*, *340*, 483–494, doi:10.1016/j.crte.2008.06.004.

Orr, J. C., et al. (2001), Estimates of anthropogenic carbon uptake from four three-dimensional global ocean models, *Global Biogeochem. Cycles*, *15*, 43–60, doi:10.1029/2000GB001273.

Patra, P. K., J. K. Moore, N. Mahowald, M. Uematsu, S. C. Doney, and T. Nakazawa (2007), Exploring the sensitivity of interannual basin-scale air-sea CO_2 fluxes to variability in atmospheric dust deposition using ocean carbon cycle models and atmospheric CO_2 inversions, *J. Geophys. Res.*, *112*, G02012, doi:10.1029/2006JG000236.

Pollard, R., P. Tréguer, and J. Read (2006), Quantifying nutrient supply to the Southern Ocean, *J. Geophys. Res.*, *111*, C05011, doi:10.1029/2005JC003076.

Raupach, M. R. (1994), Simplified expressions for vegetation roughness length and zero-plane displacement as functions of canopy height and area index, *Boundary Layer Meteorol.*, *71*, 211–216, doi:10.1007/BF00709229.

Raven, J. A., and P. G. Falkowski (1999), Oceanic sinks for atmospheric CO_2, *Plant Cell Environ.*, *22*, 741–755, doi:10.1046/j.1365-3040.1999.00419.x.

Revel-Rolland, M., P. De Deckker, B. Delmonte, P. P. Hesse, J. W. Magee, I. Basile-Doelsch, F. Grousset, and D. Bosch (2006), Eastern Australia: A possible source of dust in East Antarctica interglacial ice, *Earth Planet. Sci. Lett.*, *249*, 1–13, doi:10.1016/j.epsl.2006.06.028.

Ridgwell, A. J. (2002), Dust in the Earth system: The biogeochemical linking of land, air, and sea, *Philos. Trans. R. Soc. A*, *360*, 2905–2924, doi:10.1098/rsta.2002.1096.

Ridgwell, A. J., and A. J. Watson (2002), Feedback between aeolian dust, climate, and atmospheric CO_2 in glacial time, *Paleoceanography*, *17*(4), 1059, doi:10.1029/2001PA000729.

Rotstayn, L. D., M. D. Keywood, B. W. Forgan, A. J. Gabric, I. E. Galbally, J. L. Gras, A. K. Luhar, G. H. McTainsh, R. M. Mitchell, and S. A. Young (2009), Possible impacts of anthropogenic and natural aerosols on Australian climate: A review, *Int. J. Climatol.*, *29*, 461–479, doi:10.1002/joc.1729.

Sarmiento, J. L., T. M. C. Hughes, R. J. Stouffler, and S. Manabe (1998), Simulated response of the ocean carbon cycle to anthropogenic climate warming, *Nature*, *393*, 245–249, doi:10.1038/30455.

Sedwick, P. N., A. R. Bowie, and T. W. Trull (2008), Dissolved iron in the Australian sector of the Southern Ocean (CLIVAR SR3 section): Meridional and seasonal trends, *Deep Sea Res., Part I*, *55*, 911–925, doi:10.1016/j.dsr.2008.03.011.

Shao, Y. P., and L. M. Leslie (1997), Wind erosion prediction over the Australian continent, *J. Geophys. Res.*, *102*, 30,091–30,105, doi:10.1029/97JD02298.

Shao, Y., L. M. Leslie, R. K. Munro, P. Irannejad, W. F. Lyons, R. Morison, D. Short, and M. S. Wood (1997), Soil moisture prediction over the Australian continent, *Meteorol. Atmos. Phys.*, *63*, 195–215, doi:10.1007/BF01027385.

Shao, Y. P., J. F. Leys, G. H. McTainsh, and K. Tews (2007), Numerical simulation of the October 2002 dust event in Australia, *J. Geophys. Res.*, *112*, D08207, doi:10.1029/2006JD007767.

Shaw, E. C., A. J. Gabric, and G. H. McTainsh (2008), Impacts of aeolian dust deposition on phytoplankton dynamics in Queensland coastal waters, *Mar. Freshwater Res.*, *59*, 951–962, doi:10.1071/MF08087.

Takahashi, T., et al. (2002), Global sea-air CO_2 flux based on climatological surface ocean pCO_2, and seasonal biological and temperature effects, *Deep Sea Res., Part II*, *49*, 1601–1622, doi:10.1016/S0967-0645(02)00003-6.

Tanaka, T. Y., and M. Chiba (2006), A numerical study of the contributions of dust source regions to the global dust budget, *Global Planet. Change*, *52*, 88–104, doi:10.1016/j.gloplacha.2006.02.002.

Turner, S. M., M. J. Harvey, C. S. Law, P. D. Nightingale, and P. S. Liss (2004), Iron-induced changes in oceanic sulfur biogeochemistry, *Geophys. Res. Lett.*, *31*, L14307, doi:10.1029/2004GL020296.

Wang, M. H., S. Bailey, and C. R. McClain (2000), SeaWIFS provided unique global aerosol optical property data, *Eos Trans. AGU*, *81*, 197–202, doi:10.1029/00EO00132.

Wanninkhof, R., and W. R. McGillis (1999), A cubic relationship between air-sea CO_2 exchange and wind speed, *Geophys. Res. Lett.*, *26*, 1889–1892, doi:10.1029/1999GL900363.

Watson, A. J., D. C. E. Bakker, A. J. Ridgwell, P. W. Boyd, and C. S. Law (2000), Effect of iron supply on Southern Ocean CO_2 uptake and implications for glacial atmospheric CO_2, *Nature*, *407*, 730–733, doi:10.1038/35037561.

Weiss, R. F. (1974), Carbon dioxide in water and seawater: The solubility of a non-ideal gas, *Mar. Chem.*, *2*, 203–215, doi:10.1016/0304-4203(74)90015-2.

Wolff, E. W., et al. (2006), Southern Ocean sea-ice extent, productivity and iron flux over the past eight glacial cycles, *Nature*, *440*, 491–496, doi:10.1038/nature04614.

Zhu, X. R., J. M. Prospero, F. J. Millero, D. L. Savoie, and G. W. Brass (1992), The solubility of ferric ion in marine mineral aerosol solutions at ambient relative humidities, *Mar. Chem.*, *38*, 91–107, doi:10.1016/0304-4203(92)90069-M.

Zhuang, G., Y. Zhen, R. A. Duce, and P. R. Brown (1992), Link between iron and sulfur cycles suggested by detection of Fe(II) in remote marine aerosols, *Nature*, *355*, 537–539, doi:10.1038/355537a0.

Zhuang, G. S., J. H. Guo, H. Yuan, and X. Y. Zhang (2003), Coupling and feedback between iron and sulphur in air-sea exchange, *Chin. Sci. Bull.*, *48*, 1080–1086, doi:10.1360/02wb0205.

H. Butler, Department of Mathematics and Computing, University of Southern Queensland, Toowoomba, Qld 4350, Australia.

R. A. Cropp, A. J. Gabric, B. M. Johnston, and G. H. McTainsh, School of Environment, Griffith University, Nathan, Qld 4111, Australia. (a.gabric@griffith.edu.au)

M. Keywood, CSIRO Marine and Atmospheric Research, Private Bag 1, Aspendale, Vic 3195, Australia.

B. Tilbrook, CSIRO Marine and Atmospheric Research, GPO Box 1538, Hobart, Tas 7001, Australia.